



HOKKAIDO UNIVERSITY

Title	Cerenkov Radiation of Frequency-Doubled Light from Leaky Waveguides
Author(s)	Hayata, Kazuya; Koshiba, Masanori
Citation	北海道大學工學部研究報告, 153, 147-155
Issue Date	1990-11-29
Doc URL	https://hdl.handle.net/2115/42258
Type	departmental bulletin paper
File Information	153_147-156.pdf



Cerenkov Radiation of Frequency-Doubled Light from Leaky Waveguides

Kazuya HAYATA* and Masanori KOSHIBA*

(Received August 31, 1990)

Abstract

A new scheme for activating Cerenkov radiation of frequency-doubled light, which takes advantage of leaky waveguides, is proposed and simulated numerically. The underlying concept of this scheme is based on a possibility of increasing overlap between the fundamental (driving) and the frequency-doubled (driven) field profiles along the transverse direction. A preliminary investigation is made on the frequency doubling of infrared coherent radiation using a bent planar waveguide. Numerical results for the generated harmonic power as a function of the interaction length are shown, taking the radius of curvature of the bend as a parameter. Also displayed are the evolutionary plots of interacting fields, by which the effect of the bend on the field profile is visually understood.

1. Introduction

Growing interest in utilizing nonlinear guided-wave phenomena for applications requiring a compact blue light source with high degree of coherence is undoubtedly due to the extremely enhanced flux density and longer interaction length in comparison with the conventional bulk optics geometry. In analogy to the radiation of light from an electron moving in a material, which was initially observed by Cerenkov, frequency-doubled light can be generated at a certain angle against the propagation direction of pumping light provided that the phase-matching condition (law of conservation of momentum) is fulfilled¹⁾. In contrast to the extremely strict phase-matching requirement inherent in ordinary interaction between discrete guided modes, the advantage of this method is that the phase-matching condition between the fundamental guided mode and the frequency up-converted radiation mode can be automatically satisfied solely by adjusting waveguide parameters, indicating that no strict temperature tuning is needed. However, recent analytical and numerical studies on the Cerenkov phase matching have revealed to us that the conversion efficiency predicted is dependent on the guide parameters in a critical fashion although the dependence is far more relaxed than that predicted for the interaction between discrete guided modes²⁾⁻⁹⁾. Indeed, more recently, it has been predicted by the authors that by tailoring the nonlinear susceptibility profile along the transverse direction, considerable enhancement of the efficiency, which attains nearly one order of magnitude larger than that of the conventional

* Department of Electronic Engineering, Sapporo 060, Japan

structure, is, in principle, possible⁵⁾.

In this paper a novel scheme for activating Cerenkov radiation of frequency-doubled light, which takes advantage of a variety of field profiles that propagate down leaky waveguides, is proposed and simulated numerically with the aid of the split-step finite-element method that has been developed by the authors and to date, successfully applied to a wide scope of nonlinear optics problems such as second- and third-harmonic generations^{3),9)}, nonlinear beam propagation in an arbitrary-shaped waveguide¹⁰⁾⁻¹²⁾, and soliton dynamics in a single-mode and a birefringent glass fiber^{13),14)}. The underlying concept of this scheme is based on a possibility of increasing the overlap between the fundamental (driving) and the frequency-doubled (driven) field profiles along the transverse direction. A preliminary investigation is made on the frequency doubling of infrared coherent radiation using a bent planar waveguide. Numerical results for the generated harmonic power as a function of the interaction length are shown, taking the radius of curvature of the bend as a parameter. Also displayed are the evolutonal plots of interacting fields, by which the effect of the bend on the field profile is visually elucidated.

2. Modeling

2.1. Nonlinear wave equations

As a leaky waveguide structure we consider in this paper a bent planar waveguide with a radius of curvature, R , a section of which is schematically illustrated in Fig. 1. First, we shall derive wave equations for the problem with the global coordinate system (ρ, α, Z) . Implying second-harmonic generation (SHG), as an explicit form of the TE component of the total electric field vector we consider

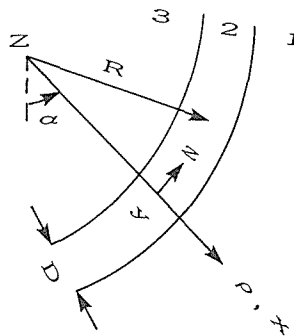


Fig. 1 Schematic sketch of a bent planar waveguide. Two coordinate systems, (ρ, α, Z) and (x, y, z) , are used to define the waveguide structure. Light propagates along the z -axis. The region 2 is a guiding film whereas the regions 1 and 3 are claddings that bound the film. D is the thickness of the film, and R is the radius of curvature of the bent waveguide.

$$E_z(\rho, \alpha, Z, t) = 1/2[\psi(\rho, \alpha, Z) \exp(j\omega t) + \psi'(\rho, \alpha, Z) \exp(j2\omega t)] + c. c. \quad (1)$$

where ψ and ψ' are the amplitudes of the fundamental and the second-harmonic (SH) waves, respectively (in this paper a prime indicates a quantity for the SH), ω is the angular frequency of the fundamental, and *c. c.* denotes a complex conjugate. Substituting Eq. (1) into source-free Maxwell's equations

$$\nabla \times \underline{E} = -\mu_0 \partial \underline{H} / \partial t, \quad \nabla \times \underline{H} = \partial \underline{D} / \partial t \quad (2)$$

and the nonlinear material equation

$$D_z = \epsilon_0(\epsilon E_z + d E_z^2), \quad (3)$$

we obtain the coupled nonlinear wave equations

$$\partial^2 \psi / \partial \bar{\rho}^2 + \bar{\rho}^{-1} \partial \psi / \partial \bar{\rho} + \bar{\rho}^{-2} \partial^2 \psi / \partial \alpha^2 + \partial^2 \psi / \partial \bar{Z}^2 + \epsilon \psi + d \psi^* \psi' = 0 \quad (4a)$$

$$\partial^2 \psi' / \partial \bar{\rho}^2 + \bar{\rho}^{-1} \partial \psi' / \partial \bar{\rho} + \bar{\rho}^{-2} \partial^2 \psi' / \partial \alpha^2 + \partial^2 \psi' / \partial \bar{Z}^2 + 4\epsilon' \psi' + 2d' \psi'^2 = 0 \quad (4b)$$

where \underline{E} , \underline{H} , and \underline{D} are the electric field, magnetic field, and electric displacement vectors, respectively, μ_0 , ϵ_0 , ϵ , and d the vacuum permeability, vacuum permittivity, relative permittivity, and second-order nonlinear optical coefficient, respectively, $\bar{\rho} = k_0 \rho$, $\bar{Z} = k_0 Z$ (k_0 : free-space wave number; $k_0 = 2\pi/\lambda_0$), and asterisk seen in the left-hand side of Eq. (4a) denotes a complex conjugate.

Using the relation between the global coordinate system, (ρ, α, Z) , and the local coordinate system, (x, y, z) ¹⁵⁾,

$$\rho = R + x, \quad Z = y, \quad \alpha = z/R \quad (5)$$

and assuming the planar condition, $\partial/\partial y \equiv 0$, we reduce Eq. (4) to

$$\partial^2 \psi / \partial \bar{x}^2 + (\bar{R} + \bar{x})^{-1} \partial \psi / \partial \bar{x} + \bar{R}^2 (\bar{R} + \bar{x})^{-2} \partial^2 \psi / \partial \bar{z}^2 + \epsilon \psi + d \psi^* \psi' = 0 \quad (6a)$$

$$\partial^2 \psi' / \partial \bar{x}^2 + (\bar{R} + \bar{x})^{-1} \partial \psi' / \partial \bar{x} + \bar{R}^2 (\bar{R} + \bar{x})^{-2} \partial^2 \psi' / \partial \bar{z}^2 + 4\epsilon' \psi' + 2d' \psi'^2 = 0 \quad (6b)$$

with $\bar{x} = k_0 x$, $\bar{y} = k_0 y$, $\bar{z} = k_0 z$, and $\bar{R} = k_0 R$.

Furthermore, to rule out contributions from the rapidly oscillating components along the propagation axis we write ψ and ψ' as

$$\psi(\bar{x}, \bar{z}) = e(\bar{x}, \bar{z}) \exp(-j\bar{\beta}\bar{z}), \quad \psi'(\bar{x}, \bar{z}) = e'(\bar{x}, \bar{z}) \exp(-j2\bar{\beta}\bar{z}) \quad (7)$$

with the automatically satisfied phase-matching requirement inherent in the Cerenkov doubling being implied, and with $\bar{\beta}$ the effective index of the fundamental wave.

Substituting Eq. (7) into Eq. (6) we finally obtain the nonlinear parametric equations to be solved numerically

$$\begin{aligned} & j2\bar{\beta}\bar{R}^2(\bar{R} + \bar{x})^{-2} \partial e / \partial \bar{z} \\ & = \partial^2 e / \partial \bar{x}^2 + (\bar{R} + \bar{x})^{-1} \partial e / \partial \bar{x} + [\epsilon(\bar{x}) - \bar{\beta}^2 \bar{R}^2 (\bar{R} + \bar{x})^{-2}] e + d(\bar{x}) \psi^* \psi' \\ & j4\bar{\beta}\bar{R}^2(\bar{R} + \bar{x})^{-2} \partial e' / \partial \bar{z} \end{aligned} \quad (8a)$$

$$= \partial^2 e' / \partial \bar{x}^2 + (\bar{R} + \bar{x})^{-1} \partial e' / \partial \bar{x} + 4[\varepsilon'(\bar{x}) - \bar{\beta}^2 \bar{R}^2 (\bar{R} + \bar{x})^{-2}] e' + 2 d'(\bar{x}) \psi^2 \quad (8b)$$

where the slowly varying envelope approximations, $|\partial^2 e / \partial \bar{z}^2| \ll |2\bar{\beta}\partial e / \partial \bar{z}|$ and $|\partial^2 e' / \partial \bar{z}^2| \ll |4\bar{\beta}\partial e' / \partial \bar{z}|$, have been employed. It should be noted that for smaller R these approximations would be invalid because of the rapid field variation caused by the increasing leakage of guiding flux.

2.2. Numerical tool

Application of the split-step procedure⁽¹¹⁾⁻⁽¹⁴⁾ based on the principle of uncoupling, which is mathematically equivalent to the operator splitting method, to Eq. (8) yields

$$A \partial e / \partial \bar{z} = B e, \quad A \partial e' / \partial \bar{z} = C \quad (9a)$$

$$A' \partial e' / \partial \bar{z} = B' e', \quad A' \partial e' / \partial \bar{z} = C' \quad (9b)$$

with

$$A = j 2 \bar{\beta} \bar{R}^2 (\bar{R} + \bar{x})^{-2}, \quad A' = 2 A \quad (9c)$$

$$B = \partial^2 / \partial \bar{x}^2 + (\bar{R} + \bar{x})^{-1} \partial / \partial \bar{x} + \varepsilon(\bar{x}) - \bar{\beta}^2 \bar{R}^2 (\bar{R} + \bar{x})^{-2} \quad (9d)$$

$$B' = \partial^2 / \partial \bar{x}^2 + (\bar{R} + \bar{x})^{-1} \partial / \partial \bar{x} + 4[\varepsilon'(\bar{x}) - \bar{\beta}^2 \bar{R}^2 (\bar{R} + \bar{x})^{-2}] \quad (9e)$$

$$C = d(\bar{x}) \psi^* \psi', \quad C' = 2 d'(\bar{x}) \psi^2 \quad (9f)$$

where B and B' are differential operators (' q numbers') whereas A , A' , C , and C' are numbers (' c numbers').

To apply the finite-element method (FEM) to Eq. (9), first we subdivide the entire cross-sectional domain (x direction) of the system into a number of small subdomains (subsystems) using second-order line elements, a single segment of which has three nodal points. Applying the FEM and the finite-difference method based on the Crank-Nicolson scheme, to the lateral (x) and the longitudinal (z) field variations, respectively, gives the following matrix equations within a short interval $i\Delta\bar{z} \leq \bar{z} < (i+1)\Delta\bar{z}$ along the propagation axis ($i = 0, 1, 2, \dots$):

$$\{e\}_{i+1} = [T]\{e\}_i + \{C/A\}_i \Delta\bar{z}, \quad \{e'\}_{i+1} = [T']\{e'\}_i + \{C'/A'\}_i \Delta\bar{z} \quad (10a)$$

with 'transfer' matrices

$$[T] = [L(\theta)]^{-1}[L(\theta - 1)], \quad [T'] = [L'(\theta)]^{-1}[L'(\theta - 1)]. \quad (10b)$$

Here θ is introduced as an artifice for controlling computational stability ($0 \leq \theta \leq 1$; $\theta = 1/2$ for the Crank-Nicolson scheme), and $\{\cdot\}$ and $[\cdot]$ indicate a vector and a matrix, respectively. The matrices $[L(s)]$ and $[L'(s)]$ ($s = \theta, \theta - 1$) involved in Eq. (10) are defined by

$$[L(s)] = [M(A)] - s \Delta\bar{z} [K((\bar{R} + \bar{x})^{-1}; \varepsilon - \bar{\beta}^2 \bar{R}^2 (\bar{R} + \bar{x})^{-2})] \quad (11a)$$

$$[L'(s)] = [M(A')] - s \Delta\bar{z} [K((\bar{R} + \bar{x})^{-1}; 4\{\varepsilon' - \bar{\beta}^2 \bar{R}^2 (\bar{R} + \bar{x})^{-2}\})] \quad (11b)$$

with

$$[K(p_1; p_2)] = \Sigma_e \{e\} (-\{N_x\}\{N_x\}^T + p_1\{N\}\{N_x\}^T + p_2\{N\}\{N\}^T) d\bar{x} \quad (11c)$$

$$[M(p_1)] = \sum_e \{p_1\} \{N\} \{N\}^T d\bar{x}. \quad (11d)$$

Here $\{N\}$ is the shape function vector for the finite elements, $\{N_x\} \equiv d\{N\}/d\bar{x}$, superscript T and subscript e denote, respectively, a transposition and each individual element, \sum_e stands for a superposition over all constituent elements that divide the entire cross-sectional domain, and p_1 and p_2 are arguments.

With $\{e\}_i$ and $\{e'\}_i$ being computed the evolutionary powers can then be evaluated by

$$P(\bar{z}) = \bar{\beta} (2 Z_0 k_0)^{-1} \{e\}_1^T [M(1)] \{e\}_1, \quad P'(\bar{z}) = \bar{\beta} (2 Z_0 k_0)^{-1} \{e'\}_1^T [M(1)] \{e'\}_1 \quad (12)$$

where Z_0 is the intrinsic impedance of vacuum, which is equal to 377 Ω . $P'(\bar{z})/P(\bar{z})$ provides the conversion efficiency for the frequency up-conversion process under consideration.

Step-by-step marching iteration of Eq. (10a) for $i=0$ (initial), 1, 2, \dots yields the evolutionary variation of the up-converted field, $e'(\bar{x}, \bar{z})$, driven by the fundamental field, $e(\bar{x}, \bar{z})$.

3. Results and discussion

To demonstrate the effect of the bend on the evolutionary variations of interacting fields we first consider a symmetric planar structure with a nonlinear film sandwiched by linear claddings. We select 2-methyl-4-nitroaniline (MNA) and SFII glasses as a core and a cladding material, respectively. MNA is one of the most nonlinear organic materials investigated to date, which has an exceptionally large second-order nonlinear optical coefficient, the largest value (d_{11}) of which is an order of magnitude greater than that (d_{33}) of LiNbO₃¹⁶. With this system the material parameters are $n_1 = n_3 = 1.7544$ and $n_2 = 1.8$ for the fundamental wavelength (1.064 μm); $n_1' = n_3' = 1.7945$ and $n_2' = 2.2$ for the SH wavelength (0.532 μm); the nonlinearity of the MNA film is given by 160 pm/V, which corresponds to d_{11} of the nonlinear tensor; and $D = 0.2 \mu\text{m}^{17}$. We subdivide the range $|x| < 20 \mu\text{m}$ into 347 line elements and 695 nodal points, and choose $\Delta z = 0.1064 \mu\text{m}$ as a longitudinally marching step. Numerical simulations are implemented with $R = 100, 10, 1,$ and 0.1 mm for a TE₀-mode input with the fundamental power of 10^4 mW/mm .

Fig. 2 show the evolutionary plots of interacting field profiles as a function of the interaction length z/λ_0 scaled by the fundamental wavelength; we choose $z=0$ as an input plane. Since no difference has been found from the plots of $R=10 \text{ mm}$, the results for $R=100 \text{ mm}$ are not displayed in Fig. 2. This indicates that the bent structures with $R > 10 \text{ mm}$ can be practically regarded as a straight one with $R = \infty$. For these structures the effective index of the fundamental wave is longitudinally invariant and is given by $\bar{\beta} = 1.7569$. With this index we can calculate the Cerenkov angle $\theta = \arccos(\bar{\beta}/n_1') = 11.7^\circ$, the value of which is in good agreement with that found directly from the simulated result [see Fig. 2(a)]. However, in bent structures with smaller R , the angle is variant along the z axis because of the longitudinally variant propagation constant. On the other hand, the field distributions are no

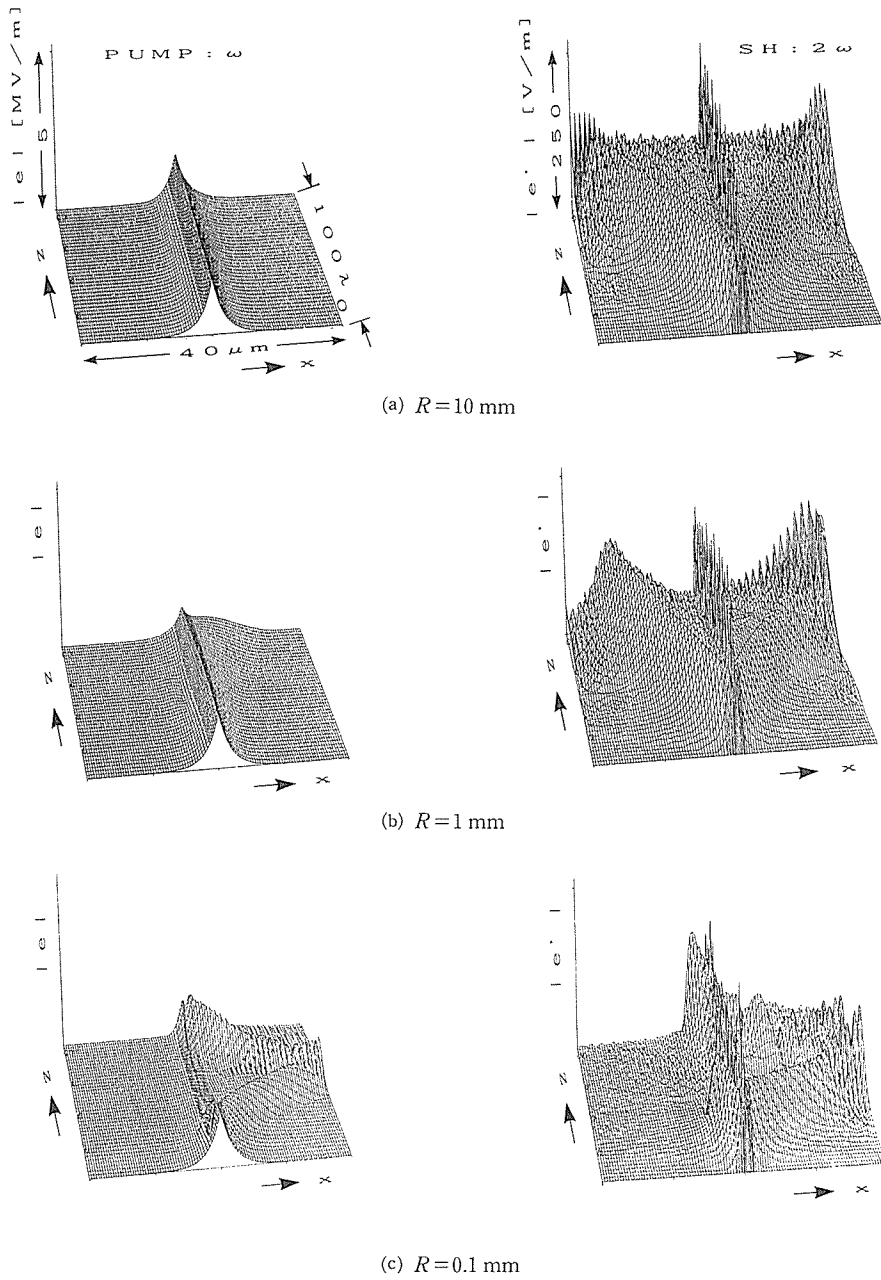


Fig. 2 Plots of evolutionary field profiles with propagation distance down a bent planar waveguide with an MNA film sandwiched by SF11 glasses. The TE_0 mode with a $1.064 \mu\text{m}$ wavelength is launched at $z=0$. In Fig. 2(c), after $50 \lambda_0$ propagation the direction of the beam propagation is reversed because of the artificial reflection of the radiated beam at the right edge of the computational window.

longer symmetric with respect to $x=0$, and deflect toward the outer region of the bend. This property could be interpreted in a good analogy to the bremsstrahlung of electromagnetic radiation due to an accelerated charged particle in the presence of the intense Coulomb field. Because of the increasing asymmetry of the pump field the cross-sectional shape of the frequency-doubled Cerenkov mode increases its asymmetry as it evolves down the guide[see Figs. 2(b) and 2(c)].

In addition to the evolutions of the field distributions we have computed the SH power as a function of the interacting length. At a $100 \lambda_0$ interaction length we have obtained as the generated power $P' = 1.1 \times 10^{-3}$, 1.1×10^{-3} , 6.9×10^{-4} , and 1.9×10^{-4} mW/mm for $R=100, 10, 1$, and 0.1 mm, respectively, indicating that no evidence for enhancement of the frequency up-conversion is found. These results suggest to us that to take advantage of the bent structure, other configurations, e. g., a linear film bounded by a nonlinear cladding¹⁸⁾, should be employed. In what follows we shall investigate the enhancement with this geometry.

Next, we consider a bent planar waveguide with a linear film bounded by a nonlinear cladding. The material parameters assumed are $n_1 = n_3 = 2.0$, $n_2 = 2.02$, $d_1 = 1$ pm/V, and $d_2 = d_3 = 0$ for the fundamental wavelength ($1.0 \mu\text{m}$); $n_1' = n_3' = 2.02$, $n_2' = 2.04$, $d_1' = d_1$, and $d_2' = d_3' = 0$ for the SH wavelength ($0.5 \mu\text{m}$); and $D = 0.317 \mu\text{m}$. As an input of the fundamental beam at $z=0$, we choose the TE_0 -mode incidence with unit pump power, 1 mW/mm. Here we do not imply any existing material. Numerical simulations have been implemented with four bends: $R=1000, 10, 5$, and 1 mm.

Table 1 Results for Cerenkov frequency doubling in a bent planar waveguide with a linear film bounded by a nonlinear cladding*

R	$C(100 \lambda_0)$	$\langle x(100 \lambda_0) \rangle$	P_1'	P_2'	P_3'	P'
1000	1.00	2.25	18.1	0.5	8.0	26.6
10	0.99	2.51	18.7	0.4	7.9	27.0
5	0.98	2.79	19.1	0.4	7.6	27.1
1	0.71	6.24	14.2	0.2	4.4	18.9

* R [mm]: radius of curvature

$C(z)$: correlation of pump beam

$\langle x(z) \rangle$ [μm]: trajectory of frequency-doubled beam

P_i' [$\times 10^{-15}$ mW/mm]: fractional powers of frequency-doubled light ($i=1, 2, 3$)

P' [$\times 10^{-15}$ mW/mm]: total power of frequency-doubled light ($P' = P_1' + P_2' + P_3'$)

Table 1 summarizes the computed results for some representative quantities. Here $C(\bar{z})$ and $\langle x(\bar{z}) \rangle$ indicate, respectively, the correlation of the fundamental beam and the trajectory of the generated SH beam, which are defined, respectively, by

$$C(\bar{z}) = \int_{-\infty}^{+\infty} |e(\bar{x}, 0)| |e(\bar{x}, \bar{z})| d\bar{x} / \left(\int_{-\infty}^{+\infty} |e(\bar{x}, 0)|^2 d\bar{x} \int_{-\infty}^{+\infty} |e(\bar{x}, \bar{z})|^2 d\bar{x} \right)^{1/2} \quad (13a)$$

$$\langle x(\bar{z}) \rangle = \int_{-\infty}^{+\infty} x |e'(\bar{x}, \bar{z})|^2 d\bar{x} / \int_{-\infty}^{+\infty} |e'(\bar{x}, \bar{z})|^2 d\bar{x}, \quad (13b)$$

for $\bar{z} > 0$ and P_i' ($i=1, 2, 3$) stand for the fractional SH powers contained within each individual domain defined in Fig. 1; consequently, the total SH power is obtained by $P' = P_1' + P_2' + P_3'$.

As expected, both the correlation and the trajectory vary more rapidly with decreasing the radius of curvature, R , because of the activated leakage of guiding flux with decreasing R . We find from the table that the former decreases with the propagation distance whereas the latter increases with the distance. In comparison among SH powers, a slight enhancement of SH radiation is found for $R=10$ and 5 mm. This observation suggests that increasing activation of the Cerenkov radiation could be achieved by bending an appropriate waveguide structure with an optimized radius of curvature.

Finally, we mention some useful applications of the bent structure, other than the increasing overlap between interacting beams by means of tailoring the transverse field profiles. In general, for weakly bent structures the propagation constant along the propagation axis is perturbed, even if the field distribution exhibits no significant variation¹⁵⁾. Utilizing this property together with the bending-induced birefringence, we can control the Cerenkov angle by purposely varying the radius of curvature of the bend. Another interesting application of the structure lies in the tunability of the strict phase-matching condition for conventional interactions between discrete guided modes, utilizing the bending-induced variation of the propagation constant. This idea would be more promising in the frequency conversion using a fiber, and may be more useful than the temperature tuning widely adopted to date.

4. Summary and Conclusions

A novel scheme for activating Cerenkov radiation of frequency-doubled light, which takes advantage of a variety of field profiles that propagate down a leaky waveguide, has been proposed and simulated numerically with the aid of the split-step finite-element method that was developed by the authors. The underlying concept of this scheme is based on a possibility of increasing overlap between the fundamental (driving) and the frequency-doubled (driven) field profiles along the transverse direction. A preliminary investigation has been made on the frequency doubling of infrared coherent radiation using a bent planar waveguide. Numerical results for the generated harmonic power as a function of the interaction length have been shown, taking the radius of curvature of the bend as a parameter. The evolutionary plots of interacting fields have also been displayed.

Acknowledgments

The authors thank K. Saka for his assistance in the numerical simulations. This work was partially supported by a Scientific Research Grant-In-Aid from the Ministry of Education, Science and Culture, Japan.

References

- 1) P. K. Tien, R. Ulrich and R. J. Martin; *Appl. Phys. Lett.* 17 (1970)447.
- 2) N. A. Sanford and J. M. Connors; *J. Appl. Phys.* 65 (1989) 1429.
- 3) K. Hayata and M. Koshiba; *Electron. Lett.* 25 (1989) 376.
- 4) K. Hayata, T. Sugawara and M. Koshiba; *IEEE J. Quantum Electron.* 26 (1990) 123.
- 5) K. Hayata, K. Yanagawa and M. Koshiba; *Appl. Phys. Lett.* 56 (1990)206.

- 6) K. Hayata, T. Sugawara and M. Koshiba ; *J. Appl. Phys.* 67 (1990) 2672.
- 7) G. Hatakoshi, K. Terashima and Y. Uematsu ; *Trans. Inst. Electron. Inform. Commun. Eng.* E73 (1990) 488.
- 8) K. Chikuma and S. Umegaki ; *J. Opt. Soc. Am. B* 7 (1990) 768.
- 9) K. Hayata, K. Yanagawa and M. Koshiba ; in *Digest of Third Optoelectronics Conference* (Institute of Electronics, Information and Communication Engineers, Tokyo, Japan, 1990), paper 13B3-11.
- 10) K. Hayata, A. Misawa and M. Koshiba ; *Electron. Lett.* 25 (1989) 661.
- 11) K. Hayata, A. Misawa and M. Koshiba ; *Trans. Inst. Electron. Inform. Commun. Eng.* J73-C-I (1990) 151.
- 12) K. Hayata, A. Misawa and M. Koshiba ; *J. Opt. Soc. Am. B* 7 (1990) 1772.
- 13) M. Eguchi, K. Hayata and M. Koshiba ; *Trans. Inst. Electron. Inform. Commun. Eng.* J72-C-I (1989) 329 ; *Electron. Commun. Jpn. Pt. 2*, 73 (1990) 81.
- 14) M. Eguchi, K. Hayata and M. Koshiba ; *Trans. Inst. Electron. Inform. Commun. Eng.* J73-C-I (1990) 113.
- 15) N. Morita, T. Tanaka and N. Kumagai ; *Trans. Inst. Electron. Commun. Eng. Jpn.* J68-B (1985) 484.
- 16) B. F. Levine, C. G. Bethea, C. D. Thurmond, R. T. Lynch and J. L. Bernstein ; *J. Appl. Phys.* 50 (1979) 2523.
- 17) M. J. Weber, ed ; "CRC Handbook of Laser Science and Technology" CRC Press, Boca Raton, Fla. (1986) Vols. III and IV.
- 18) K. Hayata, K. Yanagawa and M. Koshiba ; *Opt. Lett.* 15 (1990) 999.